

The Lupus Transit Survey for Hot Jupiters: Results and Lessons

Daniel D R Bayliss

Research School of Astronomy and Astrophysics, The Australian National University, Mount Stromlo Observatory, Cotter Road, Weston Creek, ACT 2611, Australia

daniel@mso.anu.edu.au

David T F Weldrake

Harvard-Smithsonian Center for Astrophysics, 60 Garden St MS-51, Cambridge, MA 02138, USA

dweldrak@cfa.harvard.edu

Penny D Sackett

Research School of Astronomy and Astrophysics, The Australian National University, Mount Stromlo Observatory, Cotter Road, Weston Creek, ACT 2611, Australia

penny.sackett@anu.edu.au

Brandon W Tingley

Instituto de Astrofísica de Canarias C/ Vía Láctea, s/n E38205 - La Laguna (Tenerife), Spain

btingley@iac.es

Karen M Lewis

School of Mathematical Sciences, Monash University, Clayton, Victoria 3800, Australia

karen.lewis@sci.monash.edu.au

ABSTRACT

We present the results of a deep, wide-field transit survey targeting “Hot Jupiter” planets in the Lupus region of the Galactic plane conducted over 53 nights concentrated in two epochs separated by a year. Using the Australian National University 40-inch telescope at Siding Spring Observatory (SSO), the survey covered a 0.66 deg^2 region close to the Galactic Plane ($b = 11^\circ$) and monitored a total of 110,372 stars ($15.0 < V < 22.0$). Using difference imaging photometry, 16,134 light curves with a photometric precision of $\sigma < 0.025 \text{ mag}$ were obtained. These light curves were searched for transits, and four candidates were detected that displayed low-amplitude variability consistent

with a transiting giant planet. Further investigations, including spectral typing and radial velocity measurements for some candidates, revealed that of the four, one is a true planetary companion (Lupus-TR-3), two are blended systems (Lupus-TR-1 and 4), and one is a binary (Lupus-TR-2). The results of this successful survey are instructive for optimizing the observational strategy and follow-up procedure for deep searches for transiting planets, including an upcoming survey using the SkyMapper telescope at SSO.

Subject headings: planetary systems - techniques: photometric

1. Introduction

To date, approximately 15% of all known extrasolar planets have been discovered by detecting the photometric signal produced when the planet transits its host star.¹ This transit technique offers not only a fruitful discovery mechanism, but also a means of determining the planetary radius, and with spectroscopic follow up, true planetary mass and density. Furthermore, for bright stars, the atmospheres of transiting planets can be studied, both in emission (Charbonneau et al. 2005; Deming et al. 2005) and absorption (Vidal-Madjar et al. 2004; Tinetti et al. 2007).

Wide-field transit surveys generally target bright ($V < 12$) stars, and have yielded the majority of transiting planet discoveries (for example, HATNet, Bakos et al. (2007); TrES, Alonso et al. (2004); WASP, Collier Cameron et al. (2007); and XO, McCullough et al. (2006)). Deeper, narrower surveys are less numerous in the literature, yet have also been successful, most notably the OGLE Survey (Udalski et al. 2002), which has detected several confirmed transiting planets down to $V \sim 17.0$ (Udalski 2007).

Deep surveys require larger aperture telescopes (typically ~ 1 m), and the faint candidates they produce are difficult to follow up. However, for statistical studies of extrasolar planet populations, deep surveys will grow in importance. Due to the advent of very large format, high-quality mosaic CCD cameras, the huge number of main sequence dwarfs in each field, and the improvements in follow-up techniques, large numbers of planets can be found. Deep surveys also monitor a much higher fraction of late type stars, about which less is known in terms of planetary companions.

We report here on the strategy and results from the Lupus Transit Survey, a deep survey focusing on monitoring stars in the magnitude range $14.5 < V < 19.5$ in a 0.66 deg^2 field. More than 16,000 stars were monitored with a 1m class telescope (coupled with a large format CCD detector) with sufficient precision ($\sigma < 0.025$), cadence (6 minutes), and survey duration (26 contiguous nights in 2005, 27 contiguous nights in 2006) to have high sensitivity to detect transiting Hot Jupiters out to a few days in orbital period.

¹<http://exoplanet.eu/>

The motivation for the Lupus Transit Survey was threefold. First, the survey is a deep transit search in its own right, capable of discovering interesting planetary systems in a previously unsampled part of the sky. Second, the survey acts as a control field for the previous globular cluster transit surveys of Weldrake et al. (2005, 2007), both of which produced significant null results using the same telescope, instrumental setup, and a very similar observational strategy. Third, the Lupus Survey acts as an excellent pilot study to refine further the techniques and strategies for the future 5.7 deg² SkyMapper Transit Survey (Bayliss & Sackett 2007), currently being undertaken from the same site.

We describe the observations and data reduction for the survey in Section 2. In Section 3 we set out the astrometric and photometric properties of the Lupus field. Section 4 describes the technique used to produce precise relative photometry for stars in the survey field. Section 5 outlines the analysis of the light curves to search for transiting planets and the procedure used to cull false candidates based on the survey data. Section 6 outlines how we fitted model transits to the photometry of candidates to determine the depth, duration, and center times for each candidate. Section 7 describes the follow-up spectral typing that was undertaken on promising candidates, while Section 8 describes the radial velocity measurements obtained for three candidates. Section 9 describes the importance of the extra data from 2006 in determining the candidates’ nature. Section 10 sets out the good seeing, near-infrared (near-IR) imaging we used to look for blended stars near our candidates. Our conclusions and discussion are set out in Section 11.

Our Lupus Survey detected the Hot Jupiter Lupus-TR-3b, which is described fully in Weldrake et al. (2008); only an overview is included in this paper. The survey also uncovered 494 previously unknown variable stars, which are published in a second companion paper: Weldrake & Bayliss (2008). A project to expand this survey, SuperLupus, is currently underway to search for longer period planets (Bayliss et al. 2008). A full statistical analysis for planet frequency in this field will be undertaken at the conclusion of the SuperLupus project. This paper, therefore, refrains from any statistical analysis of the planet frequency.

2. Observations and Data Reduction

2.1. The Instrumental Set-Up

The Lupus Transit Survey was undertaken using the Wide Field Imager (WFI) on the Australian National University (ANU) 40-inch telescope at Siding Spring Observatory (SSO) in New South Wales, Australia. Full details of the telescope and WFI are set out in Table 1. Although the detector was 52' on each side, throughout the survey one of the eight CCDs was not functional, reducing the area of sky monitored to 0.66 deg². A single broadband $V + R$ filter was used, covering the combined wavelength range of Cousins V and R , increasing the resulting signal-to-noise ratio (S/N) of the photometry for a fixed integration time. This same telescope and instrument configuration has been successfully employed in the two previous transit surveys of globular clusters: 47

Tuc and ω Cen (Weldrake et al. 2005, 2007).

2.2. Observational Strategy

The duration of a transit survey is critical to its prospects of success. Underestimating the required survey duration is certainly one reason why transiting planet survey yields have been lower than anticipated (Pont, Zucker, & Queloz 2006). In order to mitigate against this effect, a single field was observed intensely for two month-long periods separated by a year. An added advantage of this single-field strategy was that no time was lost in moving the telescope between fields. Such delays could have been lengthy given current pointing difficulties with the ANU 40-inch telescope. A crowded field near the Galactic plane was selected for the survey ($b = 11^\circ$). The exact survey field, centered at R.A. = $15^{\text{h}}30^{\text{m}}36.3^{\text{s}}$, decl. = $-42^\circ53'53.0''$ (J2000), in the constellation of Lupus, was chosen to maximize usable night-time hours, maintain a reasonable minimum distance from the Moon, minimize the number of bright (saturated) stars in the field, and minimize extinction from interstellar dust (Schlegel et al. 1998).

An exposure time of 300 s per image was adopted for all images. As the readout time of WFI is 50 s, a cadence of approximately 6 minutes was achieved during the observations.

2.3. Data Acquisition and Reduction

A total of 2710 $V + R$ images of the survey field were obtained over 53 nights (26 nights in 2005 and 27 nights in 2006). The full width at half-maxima (FWHM) of the stellar point spread functions (PSFs) were measured and recorded for each image. Due to the crowding in the field, only images with FWHM less than $2.2''$ were able to yield high-precision photometry, which left us with a total of 1783 images. Manual corrections to the pointing during the night ensured that image shifts on the CCD were kept to within a few pixels. This minimizes the effect of pixel-to-pixel sensitivity variations in the resulting photometry, and increases the number of usable sampled stars.

Data were reduced using standard IRAF² tasks in the MSCRED package, whereby the images were trimmed and bias, dark and flat-field corrected using calibration frames. Biases were obtained daily, and sky-flats taken at twilight and dawn when weather permitted.

²IRAF is distributed by the National Optical Astronomy Observatory, which is operated by the Association of Universities for Research in Astronomy, Inc., under cooperative agreement with the National Science Foundation.

3. Colour-Magnitude Diagram and Astrometry

In addition to the survey images, seven 10 minute exposures of the field were taken in V , R and I bands during good seeing, photometric conditions. These deeper images were used for an accurate identification of astrometric positions and colors for the stars in the survey field.

A V , $V - I$ color-magnitude diagram (CMD) was produced from these images to place the detected transit candidates onto the standard magnitude system (see Fig. 1). The survey has a saturation limit at $V \sim 14.5$, and a faint limit of $V = 22.0$ (19.4 for the transit search). The DAOPHOT-derived errors and calibration uncertainty (see the following paragraph) in our magnitude determinations are also overplotted, along with the location of our six transit candidates.

The CMD was calibrated via observations of MarkA standard stars (Landolt 1992; Stetson 2000) taken during the 2005 observing run in photometric conditions. More than four hundred standards were identified via matching of astrometry³. The mean and standard deviation of the magnitude shift was determined for each CCD and each filter independently. The resulting calibration uncertainty is 0.03 mag in V and 0.05 mag in $V - I$. As an additional check, the CMD was also cross-correlated with 2000 stars within $20'$ of the Lupus field center in the NOMAD online catalog⁴ and found to match within the precision of the catalog.

The astrometry for all sampled stars was determined via a search of the USNO CCD Astrometry Catalog (UCAC1), cross-identifying astrometric standard stars within the field. Several hundred such stars per CCD were successfully identified, producing an accurate determination of the astrometric solution for the stars in each CCD independently; the resulting astrometric calibration accuracy was $0.25''$. The layout of the field, with the astrometry of all the stars, can be seen in our companion paper (Weldrake & Bayliss 2008).

4. Photometry

An application of difference imaging analysis (DIA), originally described as the optimal PSF-matching package of Alard & Lupton (1998), was used to produce precise time-series photometry for each star. A modified form of this package was used (Wozniak 2000).

DIA matches the stellar PSF throughout a large database of images, thereby dramatically reducing the systematic effects from varying atmospheric conditions on the output photometric precision. This method allows ground-based observations the best prospects of detecting small-amplitude brightness variations in faint targets. DIA is an excellent method to obtain photometric time series in crowded fields as a large number of pixels are used to characterize PSF differences,

³MarkA astrometry and photometry downloaded from <http://www4.cadc-ccda.hia-ihp.nrc-cnrc.gc.ca/community/STETSON/standa>

⁴<http://www.nofs.navy.mil/data/fchpix/>

improving the PSF-matching process.

Initial stellar flux measurements via DIA are made from profile-fitted photometry on a template frame, produced by median-combining a number of the best-quality images with small offsets, in this case, 74 images with offsets ≤ 20 pixels ($8''$ on the sky or 2% the width of a CCD). Flux measurements on this template are used as the zero point of the resulting differential stellar time series for each individual star.

Stellar positions were found on a best-seeing reference image, and all the subsequent images, including the template, were then registered to these positions. The best PSF-matching kernel was determined and each registered image was subsequently subtracted from the template. The residuals from this method are dominated by photon noise. Any object that changed brightness between the image in question and the template was recorded as a bright or dark spot in the residual map.

This method of differential photometry produces a time series in differential flux counts rather than in the usual magnitude units. To convert to a standard magnitude system, we measured the total counts for each star on the template frame using the DAOPHOT/PSF package in IRAF, with the parameters set to the same values used in the DIA routine. We then converted the time-series photometry into magnitude units by the relation

$$\Delta m_i = -2.5 \log[(N_i + N_{ref,i})/N_{ref,i}],$$

where $N_{ref,i}$ is the total flux of star i on the template image, and N_i is the original difference flux in the time-series as produced with the photometry code. It is important to note when combining differential fluxes with DAOPHOT-derived reference image photometry, we must correct for errors based on the individual apertures used, as described in Appendix B of Hartman et al. (2004). An aperture correction was used to determine the scaling between the two fluxes, which was performed on the stellar DAOPHOT magnitudes. Our PSF magnitudes were consistently 0.06 mag brighter than the aperture-derived values (using the same aperture values as in the differential photometry). We hence shifted our magnitude zero point to $25.0 - 0.06 = 24.94$. This correction ensures that the differential imagery output is accurately represented in magnitude units.

Since the Lupus Transit Survey data were obtained over 53 nights in classical observing mode, our observations span a wide range of airmasses, weather conditions, and phases of the Moon. All of these effects produce systematic trends in the light curves, along with other higher order systematic effects contributing to the so-called “red” noise. The SYSREM algorithm (Tamuz et al. 2005) was used in order to reduce these systematic trends in our data set. This principle-component technique algorithm is often used in large transit surveys to remove effects in the light curves that may be common to a large data set of stars. Using only nonvariable stars in the algorithm, and running 10 iterations, an average improvement of $\sim 50\%$ in the photometric precision was achieved. The improvement was greatest for the bright stars, whose photometry is dominated by systematics as opposed to faint stars whose scatter is dominated by photon noise. This is significant, since the

survey is most sensitive to detecting planet transits against bright stars.

A total of 16,134 light curves in the field displayed post-SYSREM standard deviations (rms) of less than 0.025 mag, and it was these light curves we analyzed for transiting planets. The total data set of 110,372 light curves was analyzed only for large-scale variability. A total of 494 previously unknown variable stars were identified in the field; these have been published by Weldrake & Bayliss (2008).

Figure 2 shows the photometric precision achieved for those stars with $15.0 < V < 19.4$, which includes the 16,134 stars analyzed for transiting planets. The overplotted solid line shows the total of the theoretical photon noise for the star and sky, which describes the photometry well.

5. Transit Search and Candidate Selection

Since the primary goal for the Lupus Survey was the discovery of transiting Hot Jupiters, immediately after the 2005 observing run, we searched for transitlike events in the 2005 data set. As the field was only visible for follow-up work for \sim three months after the observing run, it was important to identify candidates as soon as was possible. After the 2006 observing run, the combined data set was searched again; the results of this are discussed in Section 9.

The Box-fitting Least-Squares (BLS) algorithm (Kovács, Zucker, & Mazeh 2002) was used to search for transit signals in our light curves. The BLS algorithm searches for the first-order shape of a transit via least squares fitting of step functions to the phase-wrapped data, and is widely used in transit surveys.

For each light curve, BLS was used to compute the best period and a corresponding significance of that period, the so-called Signal Detection Efficiency (SDE). Light curves were ranked according to their SDE, and all were examined wrapped at the BLS determined best-fit period and integer aliases thereof.

From the 2005 data, four candidates were identified with high SDE and phase-wrapped light curves consistent with that expected for a transiting Hot Jupiter (see Fig. 3). Two further candidates, Lupus-TR-5 and Lupus-TR-6 showed transitlike signals, (see Fig. 3), however inspecting the raw images revealed that both were on, or very close to, defective columns on the CCD. We conclude that the low level signal we detected in these candidates is due to systematic effects as they drift over the defective CCD column during the course of the observations, and we do not discuss these candidates further.

The four promising candidates and their properties (R.A., decl., V mag and $V - I$ color) are set out in Table 2. Figure 3 shows the phase-wrapped $V + R$ photometry (with open circles for the 2005 data, filled circles for 2006). The best-fitting transit model (see Section 6) is also overplotted for each. Figure 4 similarly shows the photometry for the time of anti-transit for Lupus-TR-1 and Lupus-TR-2, described further in Section 9.

For each candidate the total signal to noise for the transit feature was calculated using the equation:

$$S/N = d\sqrt{n_t}/\sigma,$$

where σ is the out-of-transit rms for the lightcurve, d is the transit depth (both in magnitude units), and n_t is the number of in-transit points in the light curve. In addition, the number of observed transits for each candidate was determined as a measure of robustness.

The η diagnostic (Tingley & Sackett 2005) was calculated for each candidate to help weed out the most likely astrophysical false positives. The diagnostic η is a measure of how consistent the transiting candidate’s depth, period, and duration are with the expected theoretical values for a transiting extrasolar planet.

The results for the S/N, number of observed transits, and η diagnostic are set out in Table 3. By way of comparison, the Lupus candidate diagnostic numbers are plotted with those of the confirmed OGLE planets (as of 2007) in Figure 5. We note that Lupus-TR-1 and TR-4 have η higher than most of the OGLE planets, increasing the likelihood that they are false positives. Lupus-TR-3 alone has an η value comparable to the OGLE planets.

Careful examination of the images allowed us to show that Lupus-TR-4 was probably not planetary in origin without the need for follow-up observations. Lupus-TR-4 had a close neighbor, which had already been identified as an eclipsing binary system as part of our search for variable stars in the field (Weldrake & Bayliss 2008). Upon inspection it was found that the period and phase of Lupus-TR-4 matched that of its eclipsing binary neighbor, although with a far lower amplitude, which gave it a depth consistent with a planetary transit. We conclude that the signal seen in Lupus-TR-4 is the result of blending with its neighbor. This still left three promising candidates (Lupus-TR-1, TR-2, and TR-3) which warranted further follow-up work.

6. Transit Fitting

To determine the parameters of the detected candidates, a transit fitting algorithm was developed. This algorithm uses the transit models of Mandel & Agol (2002) to determine the best-fitting set of system parameters for a fixed orbital period (and quadratic limb-darkening coefficients appropriate for the spectral type of the primary), using a minimization of the rms between the data and the model as a fit statistic.

For each candidate, a large number of transit models are produced ($\sim 100,000$) for various stellar radii, orbital inclinations and planet radii for a fixed orbital period and stellar mass appropriate to the respective spectral type (see Section 7). The orbital semimajor axis is determined from these parameters, with the exact range of model parameters dependent on the grazing/equatorial appearance of the transit itself. Each individual model is then compared to the phase-wrapped photometry (in units of hours from transit center time) and a resulting rms residual is obtained.

The model with the lowest residual is taken as the best-fitting description of the data. The fits are displayed as solid lines overplotted on the photometry in Figure 3. From this best fit, we derive the maximum transit depth (d) and the duration for transit (T_{14}) for each candidate (see Table 3).

Uncertainties, also seen in Table 3 were determined via bootstrap resampling. A variation on this fitting program was used to determine the transit center times (T_C), also seen in Table 3. Here we took the best-fitting transit model for each candidate, comparing it to a well-sampled single unphase-wrapped transit and determined the corresponding transit center time that minimizes the residuals. Uncertainties were again determined via bootstrap resampling.

7. Spectral Typing

Spectra were obtained for the remaining candidates, Lupus-TR-1, TR-2, and TR-3, using the Double Beam Spectrograph (DBS) on the ANU 2.3 m telescope at SSO. For Lupus-TR-1 and Lupus-TR-2 the 600-line blue grating was used, which gives resolution of 400 over a wavelength range of 3600-4800 Å (Fig. 6). For Lupus-TR-3, a 300-line blue grating was used, yielding a resolution of 200 over 4000-6700 Å (Fig. 7).

The spectra were reduced using standard IRAF tasks. Corrections for interstellar reddening assumed $E(B-V)=0.182$, an estimate based on dust maps of the survey field (Schlegel et al. 1998). The reduced spectra were then compared to the extensive MILES library of empirical spectra (Sánchez-Blázquez et al. 2004), chosen as a comparison set as it closely matched the spectral resolution we obtained for our candidates.

Comparison to the MILES library indicated that both Lupus-TR-1 and Lupus-TR-2 are early G-type dwarf stars, while Lupus-TR-3 is an early K-type dwarf (see Figs. 6, 7, and Table 2). Since none of these three candidates are giant stars, we can rule out the possibility of a very large radius star being transited by a nonplanetary secondary or a giant star blending a stellar eclipsing system as the cause of the $\sim 1\%$ dip.

8. Radial Velocity measurements

RV measurements provide the ultimate verification as to whether a candidate transit is caused by an orbiting planet by determining the mass of the transiting object, which in turn defines whether the object is stellar or planetary in nature.

RV followup is a major hurdle for deep transit surveys, and typically requires significant amounts of time on 8m class telescopes to produce high-resolution spectra with sufficient signal to noise for accurate RV cross-correlation. The three promising Lupus candidates range from $V=14.6$ to $V=17.4$. In an effort to make best use of large aperture access, two different instruments were used to obtain sufficiently precise RV measurements for the determination of the nature of the

transiting object.

8.1. Radial Velocities from the AAT: Lupus-TR-1 and TR-2

Lupus-TR-1 and Lupus-TR-2 are at the bright end of our survey ($V \approx 14.5$), which meant that velocity measurements for these candidates could be obtained using the 3.9m Anglo-Australian Telescope (AAT) at SSO. On 2006 July 19 and 20, we obtained data in service time using UCLES, a high resolution echelle spectrograph at the AAT, without the iodine cell. The data were taken with a central wavelength of 5414\AA and a resolution of $R \approx 25,000$. The spectra cover the wavelength range of $4450\text{--}7340\text{\AA}$ in 48 orders. With 20 minute exposures, S/N of 8 per pixel was achieved.

In addition, spectra were obtained for the bright RV standard HR4695 on the same nights with the same setup. Standard tasks in the IRAF package ECHELLE were used to reduce the spectra, and wavelength calibration was performed using a number of ThAr arc lamp frames taken over the course of the observations. In total, 10 spectra were obtained for Lupus-TR-1 and nine spectra for Lupus-TR-2. We cross-correlated these spectra against the HR4695 spectrum, selecting 40 orders with sufficient S/N and a lack of strong telluric lines.

The RV for Lupus-TR-1 show no variation within the precision of our measurements, as shown in Figure 8. The service time observing we acquired fell between the predicted times of maximum and minimum RV amplitude, however on July 20 we obtained RV measurements over approximately 4 hr, which is a significant fraction of the period of Lupus-TR-1. Given that the spectral typing of this star suggests it is an early-type G-dwarf, then the lack of RV variations over this period means that we can rule out a binary companion with a mass greater than approximately $10M_J$. However, high-resolution imaging with PANIC on Magellan (see Section 10) indicates this system is most likely a blend. The final RVs for Lupus-TR-1 are given in Table 4.

The data for Lupus-TR-2 showed a discrete jump of 46 km s^{-1} over the course of just 80 minutes. We believe that this must have been due to a pointing error during the service observations, and therefore the RV measurements for Lupus-TR-2 were discarded. However further photometric monitoring of Lupus-TR-2 revealed it to be a detached eclipsing binary (see Section 9).

8.2. Magellan Radial Velocity: Lupus-TR-3

The most promising candidate, Lupus-TR-3, was too faint ($V = 17.4$) for suitable spectra to be obtained using UCLES on the AAT, and therefore high-resolution spectra for its RV measurements were obtained using the MIKE echelle spectrograph on Magellan II (Clay). A signal of $K = 114 \pm 25 \text{ m s}^{-1}$ was detected, which, along with extensive blend modeling, indicated that Lupus-TR-3 is transited by a Hot Jupiter with a mass of $0.81 \pm 0.18M_J$. Transit fitting provides a planetary radius of $0.89 \pm 0.07R_J$, hence a Jupiter-like density of $1.4 \pm 0.4 \text{ g cm}^{-3}$. These observations and results are

fully detailed in Weldrake et al. (2008). This constitutes the faintest ground-based detection of a transiting planet to date.

IR imaging of Lupus-TR-3 has very recently been obtained using PANIC on Magellan, and these data are currently being analyzed using a powerful image deconvolution technique (see Sackett et al. (2008)).

9. The Added Value of the 2006 Data

Lupus-TR-1, TR-2, and TR-3 were initially detected from the 2005 data alone. In the case of Lupus-TR-2, the 2005 light curve did not contain any data points at phase=0.5 (where phase=0 is the mid-point of the transit). However, the additional 27 nights of data taken in 2006 May/June did cover this phase region, and revealed a “secondary” eclipse, which confirmed that Lupus-TR-2 was a detached eclipsing binary system (see Fig. 4) with twice the originally estimated period. The eclipse seen at phase 0.5 is deeper than the original eclipse which was detected, meaning that we had actually seen the shallow secondary transit in 2005, but by chance missed the deep primary eclipse.

Lupus-TR-1 also exhibited a very shallow (0.8 mmag) secondary eclipse in the combined 2005/2006 data set (see Fig. 4). This is indicative of a blended eclipsing binary, and this hypothesis was subsequently examined with good-seeing, Y -band imaging (see Section 10).

Lupus-TR-3 showed no secondary eclipse in the full 2005/2006 data set. More transits of Lupus-TR-3 were observed in 2006 however, which improved our knowledge of the period and phase of this planetary host.

10. Y Band Imaging

Good-seeing (0.65”), near-IR Y -band snapshots were obtained using PANIC on Magellan I (Baade) to further help us determine the nature of Lupus-TR-1 and further examine Lupus-TR-3. This imaging of Lupus-TR-1 revealed a neighbor at approximately 2.3” from the candidate (see Figure 9). Coupled with the 0.8mmag secondary eclipse (see Fig. 4), no measured RV variations and a high η diagnostic, we conclude that this candidate is a blended eclipsing binary.

11. Summary and Conclusions

We have performed a deep search for transiting short-period giant planets in a single 0.66 deg² field above the Galactic plane ($b \sim 11^\circ$) using the ANU 40-inch telescope. Out of 16,134 stars with sufficient photometric precision (≤ 0.025 mag), we identified four transit candidates (Lupus-

TR-1 through TR-4, with $V = 14.6 \rightarrow 17.4$). Without follow-up observations, we determined that Lupus-TR-4 was a false positive as its light curve was contaminated by a nearby variable.

Of the remaining three candidates, one (Lupus-TR-2) showed a deep “secondary” eclipse when we obtained further data in 2006, revealing that the signal originally detected in the first year was in fact the secondary eclipse of a detached eclipsing binary star.

Lupus-TR-1 showed no RV variations, which coupled with the spectral typing of the primary (G1V) ruled out a grazing binary system. However, at a phase of 0.5 the light curve did show the hint of a 0.8 mmag secondary eclipse. IR images from PANIC on Magellan revealed a relatively bright neighbor, which strongly indicates this candidate is blended with an eclipsing stellar binary that causes the transit signal. Lupus-TR-3 ($V = 17.4$) was found to be the host of a hot Jupiter planet, published separately in Weldrake et al. (2008).

Candidates produced by this survey lie at the faint end of what is feasible for obtaining precise RV follow up to confirm planets and derive their mass. The difficulties of follow up in this faint regime are well outlined in Pont et al. (2008), where a program to study OGLE candidates is discussed. Similar difficulties will also be experienced by transiting planet surveys searching for low mass planets, such as *CoRoT* and *Kelper*.

In an attempt to minimize these difficulties, the upcoming SkyMapper Transit Survey (Bayliss & Sackett 2007) will be designed to monitor stars brighter than $V \sim 17$, with target numbers kept high by a combination of SkyMapper’s wide field of view and a multifield observational strategy.

The Lupus Transit Survey benefited greatly from imaging the same field in 2005 and 2006, as this produced more complete phase coverage, particularly for near integer-day periods preferentially found by ground-based surveys. It also allowed us to more accurately determine periods, which from the 2005 data alone were often confused by aliasing. This successful technique of several long, intense but widely separated epochs will be adopted in the SkyMapper Transit Survey.

The good-seeing, near-IR imaging we obtained for candidates was a relatively efficient method of checking for near neighbors that could be blended eclipsing binaries or single stars that could cause an overestimation in the flux from the primary star. Such imaging will form part of the SkyMapper Transit Survey procedure of investigating the best candidates.

Lupus-TR-5 and Lupus-TR-6 showed promising transit-shaped dips in their light curves, but were actually caused by a slight defect in the CCD. Mapping of any defects in the CCD will allow the early identification of these types of impostors, and such mapping will be implemented for the SkyMapper Transit Survey.

During the follow up of candidates from the Lupus Transit Survey, we utilized the facilities available at SSO, namely the ANU 2.3m telescope for spectral typing and the AAT for medium-precision RV measurements ($\sim 150 \text{ m s}^{-1}$ on $V \sim 15$ targets). The success of these facilities for this spectroscopic work indicates that they could be important in follow up for other transit surveys in the Southern Hemisphere.

The authors thank Grant Kennedy for his assistance in obtaining the survey data and Ken Freeman for his assistance in obtaining the spectrum of Lupus-TR-3. We acknowledge financial support from the Access to Major Research Facilities Programme, which is a component of the International Science Linkages Programme established under the Australian Government’s innovation statement, Backing Australia’s Ability.

Facilities: Magellan:Clay (MIKE), Magellan:Baade (PANIC), SSO:1m (WFI), ATT (DBS)

REFERENCES

- Alard, C., & Lupton, R. H. 1998, *ApJ*, 503, 325
- Alonso, R., et al. 2004, *ApJ*, 613, L153
- Bakos, G. Á., et al. 2007, *ApJ*, 656, 552
- Bayliss, D. D. R., & Sackett, P. D. 2007, in *ASP Conf. Ser. 366, Transiting Extrasolar Planets Workshop* ed C. Afonso, D. Wel Drake, & Th. Henning (San Francisco, CA: ASP), 320
- Bayliss, D. D. R., Sackett, P. D., & Wel Drake, D. T. F. 2008, in *IAU Symposium 253, Transiting Planets*, in press (arXiv:0807.0469v1)
- Charbonneau, D., et al. 2005, *ApJ*, 626, 523
- Collier Cameron, A., et al. 2007, *MNRAS*, 375, 951
- Deming, D., Seager, S., Richardson, L. J., & Harrington, J. 2005, *Nature*, 434, 740
- Hartman, J. D., Bakos, G., Stanek, K. Z., & Noyes, R. W. 2004, *AJ*, 128, 1761
- Kovács, G., Zucker, S., & Mazeh, T. 2002, *A&A*, 391, 369
- Landolt, A. U. 1992, *AJ*, 104, 340
- Mandel, K., & Agol, E. 2002, *ApJ*, 580, L171
- McCullough, P. R., et al. 2006, *ApJ*, 648, 1228
- Pont, F., Zucker, S., & Queloz, D. 2006, *MNRAS*, 373, 231
- Pont, F., et al. 2008, *A&A*, 487, 749
- Sackett, P. D., Gillon, M., Bayliss, D. D. R., Wel Drake, D. T. F., Tingley, B. W. 2008, in *IAU Symposium 253, Transiting Planets*, in press
- Sánchez-Blázquez, P., Peletier, R. F., Jiménez-Vicente, J., Cardiel, N., Cenarro, A. J., Falcón-Barroso, J., Gorgas, J., Selam, S., & Vazdekis, A. 2006, *MNRAS*, 371, 703

- Schlegel, D. J., Finkbeiner, D. P., & Davis, M. 1998, *ApJ*, 500, 525
- Stetson, P. B. 2000, *PASP*, 112, 925
- Tamuz, O., Mazeh, T., & Zucker, S. 2005, *MNRAS*, 356, 1466
- Tinetti, G., et al. 2007, *Nature*, 448, 169
- Tingley, B., & Sackett, P. D. 2005, *ApJ*, 627, 1011
- Udalski, A., et al. 2002, *Acta Astron.*, 52, 1
- Udalski, A. 2007, in *ASP Conf. Ser. 366, Transiting Extrasolar Planets Workshop* ed C. Afonso, D. Weldrake, & Th. Henning (San Francisco, CA: ASP), 51
- Vidal-Madjar, A., et al. 2004, *ApJ*, 604, L69
- Weldrake, D. T. F., & Bayliss, D. D. R. 2008, *AJ*, 135, 649
- Weldrake, D. T. F., Bayliss, D. D. R., Sackett, P. D., Tingley, B., Gillon, M., & Setiawan, J. 2008, *ApJ*, 675, L37
- Weldrake, D. T. F., Sackett, P. D., & Bridges, T. J. 2007, *AJ*, 133, 1447
- Weldrake, D. T. F., Sackett, P. D., Bridges, T. J., & Freeman, K. C. 2005, *ApJ*, 620, 1043
- Weldrake, D. T. F., & Sackett, P. D. 2005, *ApJ*, 620, 1033
- Wozniak, P. R. 2000, *Acta Astron.*, 50, 421

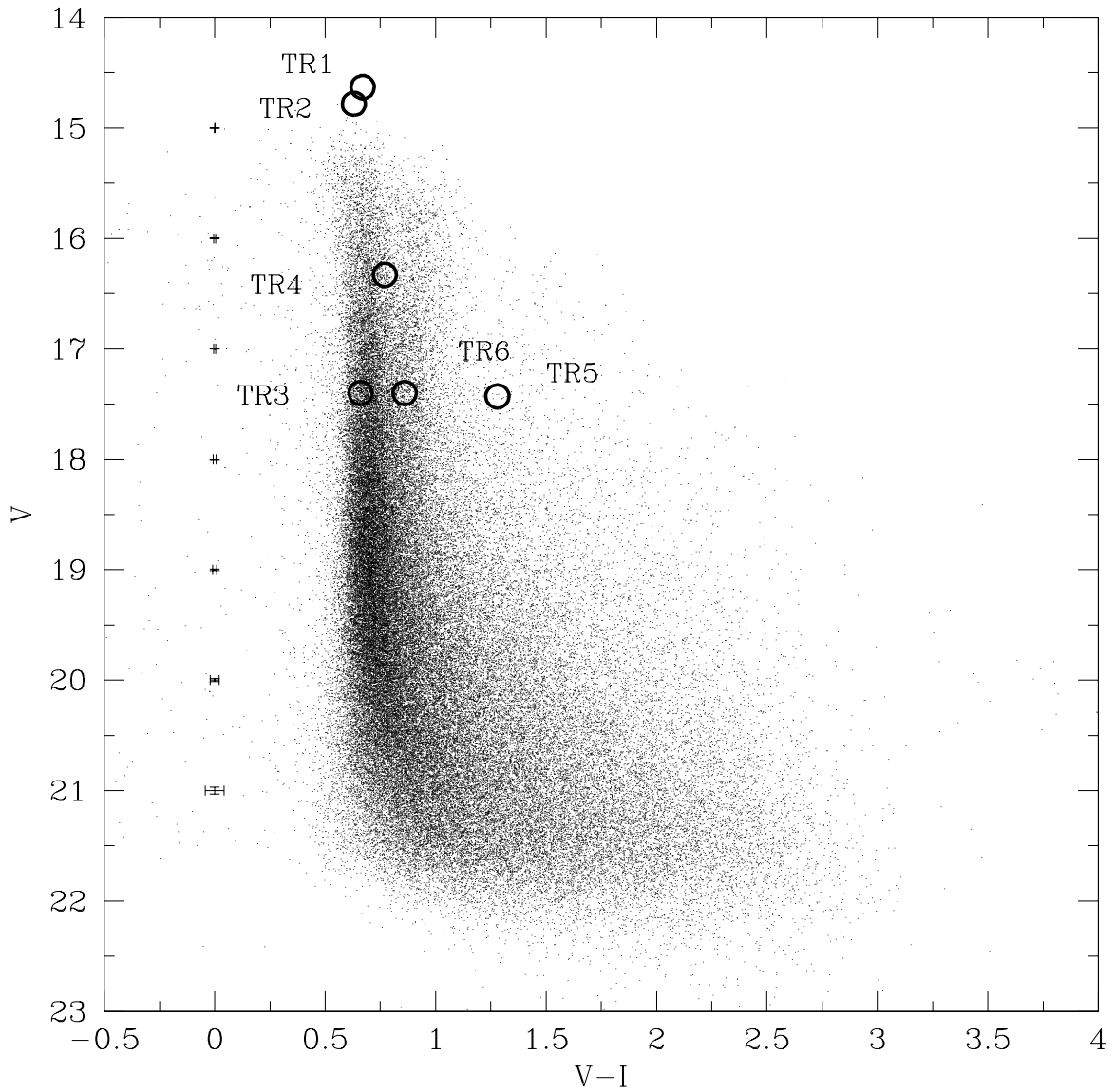


Fig. 1.— CMD for 95,358 stars in the Lupus Transit Survey field. The overplotted error bars represent the output DAOPHOT errors in the magnitudes and the CMD calibration uncertainty added in quadrature. The positions of the six transiting planet candidates in Lupus are marked with open circles and labeled.

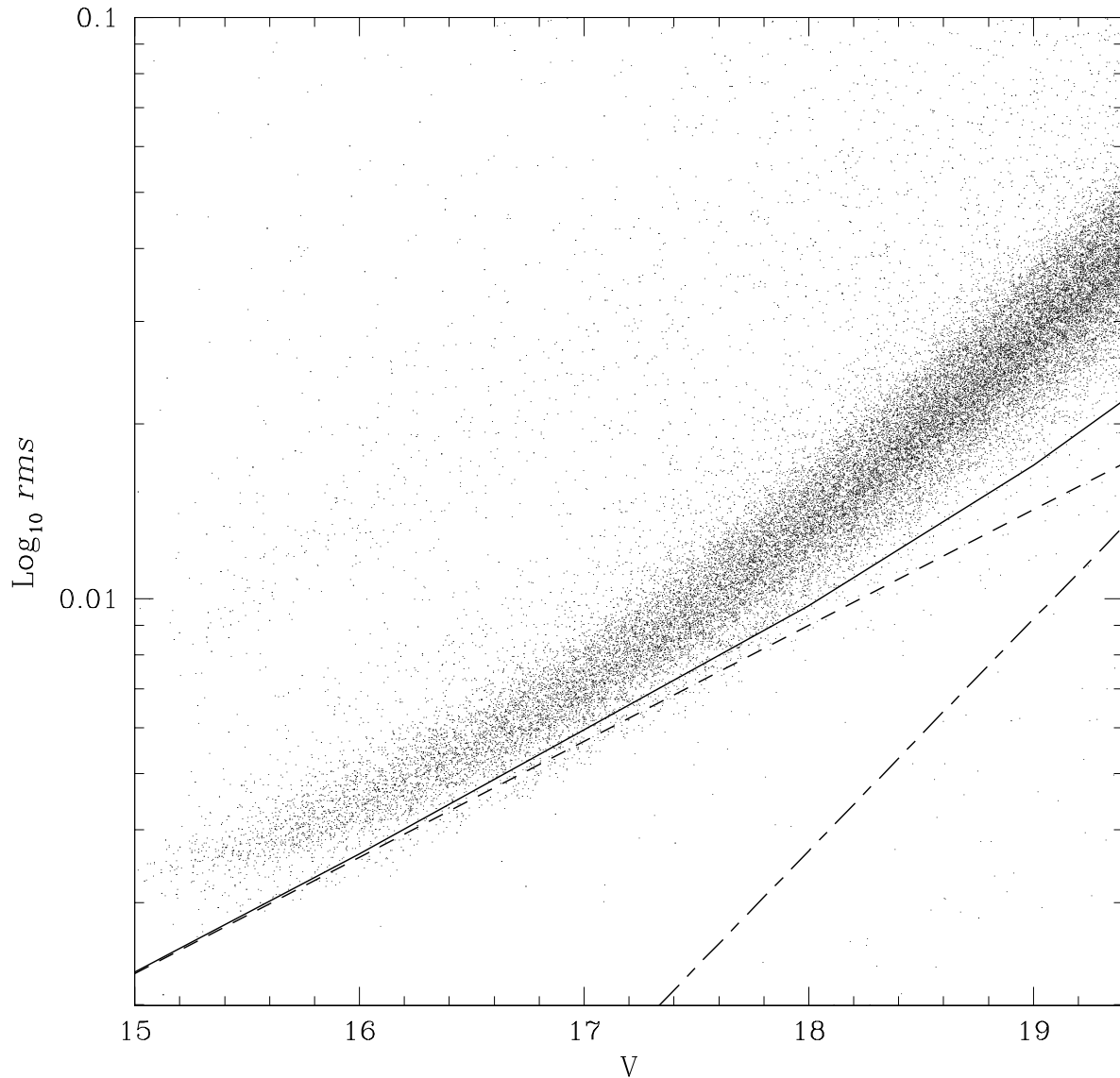


Fig. 2.— Photometric precision achieved for the stars monitored in the Lupus Transit Survey to a V magnitude limit of 19.38. The dashed line represents the photon noise from the star. The dash-dotted line represents photon noise from the sky background. The solid line is the sum of these two lines (the total photon noise). 16,134 of these stars gave light curves with an (rms) of less than 0.025 mag, and these were the stars analyzed for transiting planets.

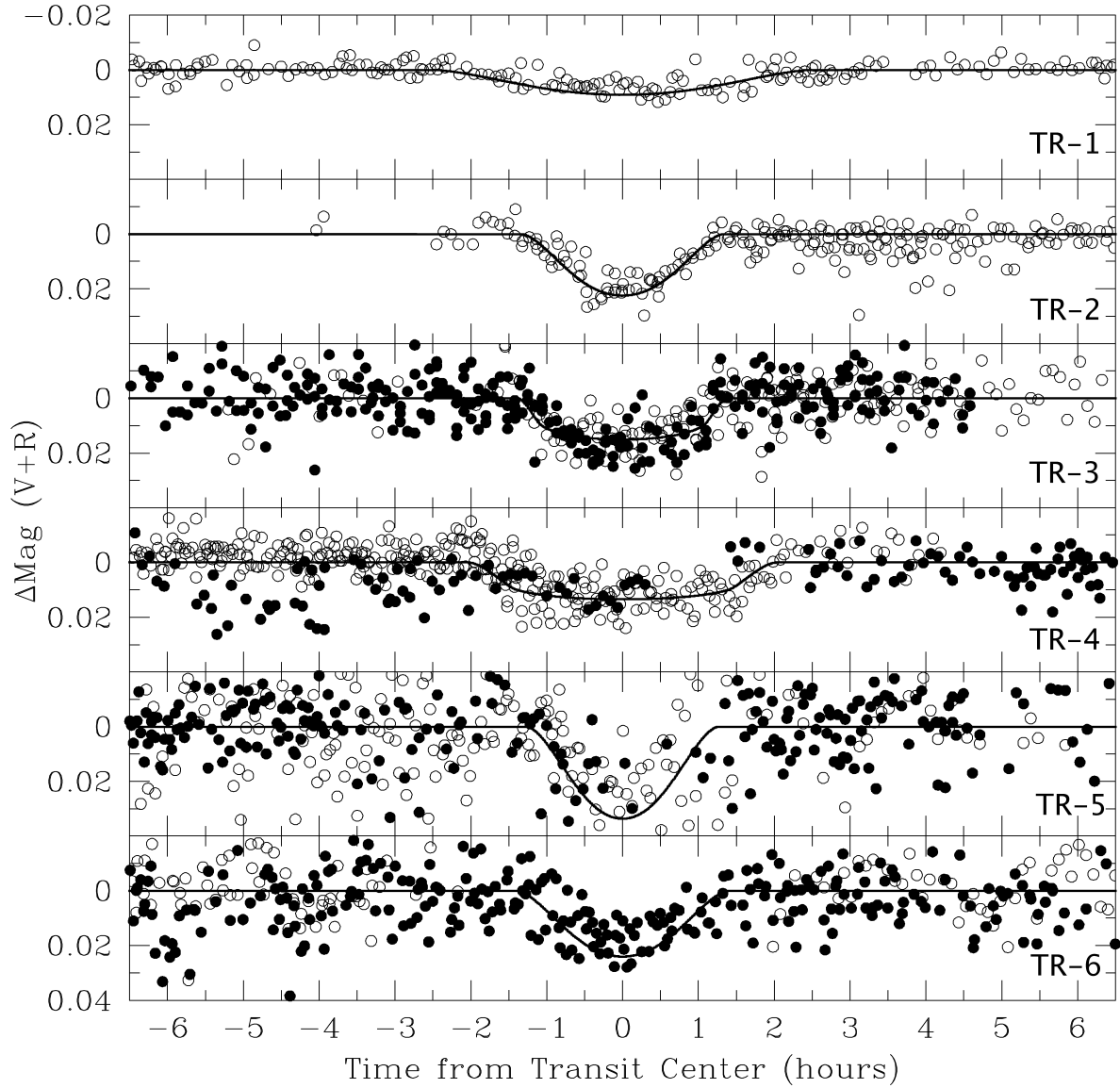


Fig. 3.— Light curves of the six transit candidates (Lupus-TR-1 at the top, in order to Lupus-TR-6 at the bottom). The open circles represent 2005 data and the filled circles represent data from 2006. The best fitting model transit is overplotted as a solid line. Lupus-TR-1 and TR-2 are both close to the saturation limit, and in 2006 (due to the mirror being re-silvered), they were saturated in most frames, thus new data were not obtained.

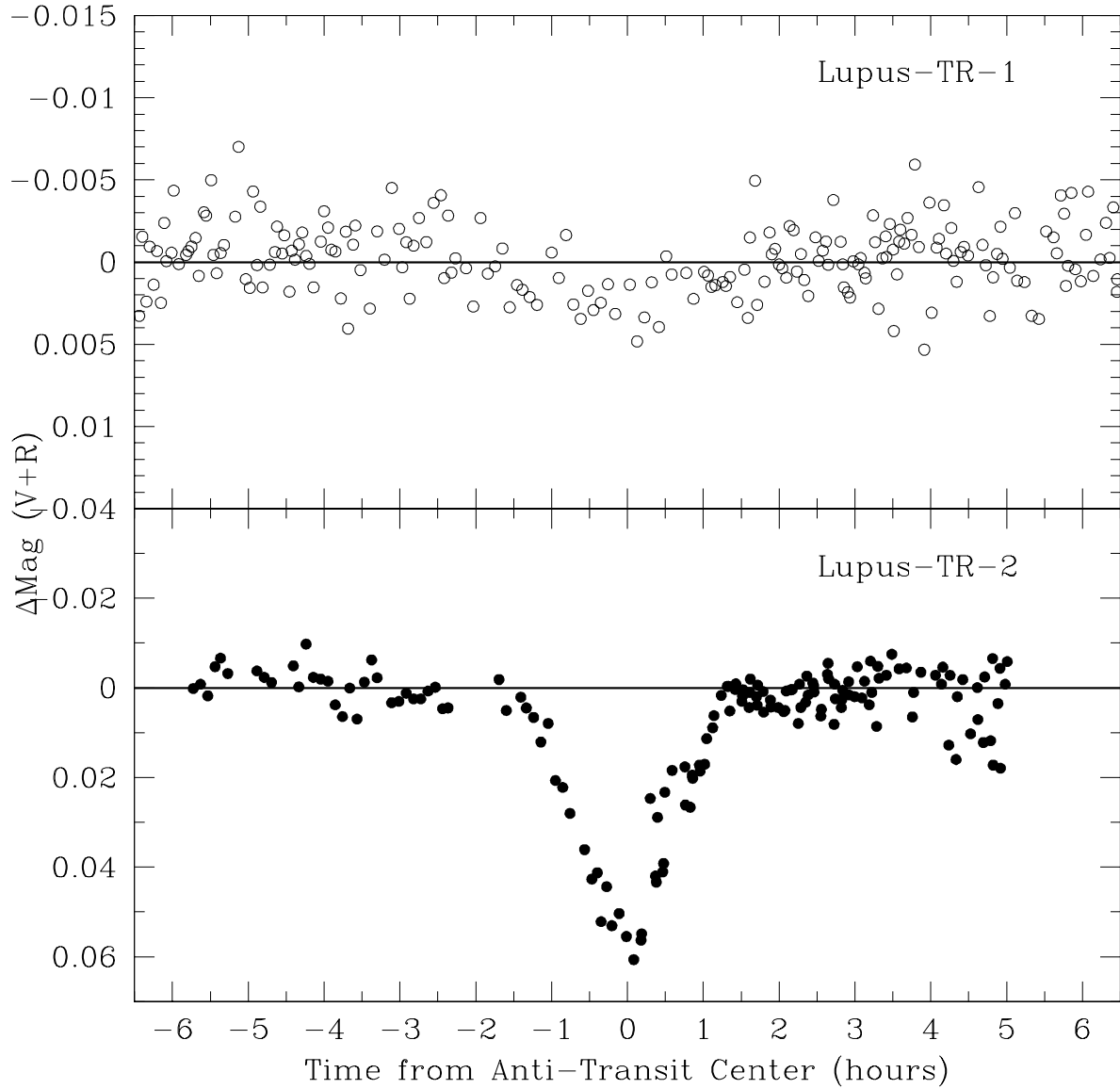


Fig. 4.— $V + R$ photometry showing the secondary eclipse of Lupus-TR-1 (top) and Lupus-TR-2 (bottom). Again the open circles represent 2005 data and the filled circles represent 2006 data. Lupus-TR-1 shows a 0.8 mmag secondary eclipse. Lupus-TR-2 shows a large 6% “secondary eclipse”, which was not seen in the 2005 data. Lupus-TR-2 is therefore a detached eclipsing binary.

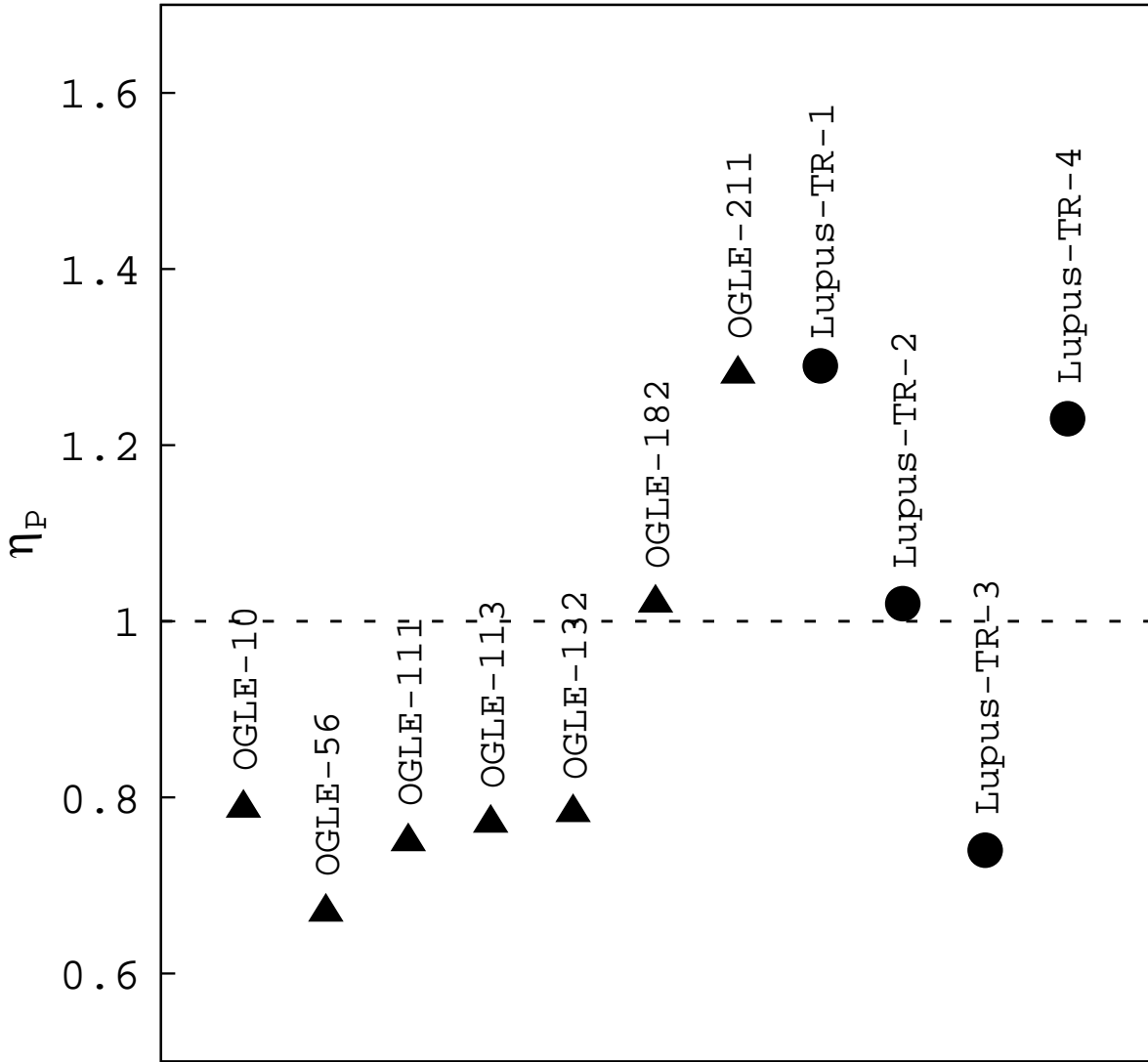


Fig. 5.— Diagnostic number (η_p) for the Lupus candidates (circles) and, for comparative purposes, the OGLE planets (triangles).

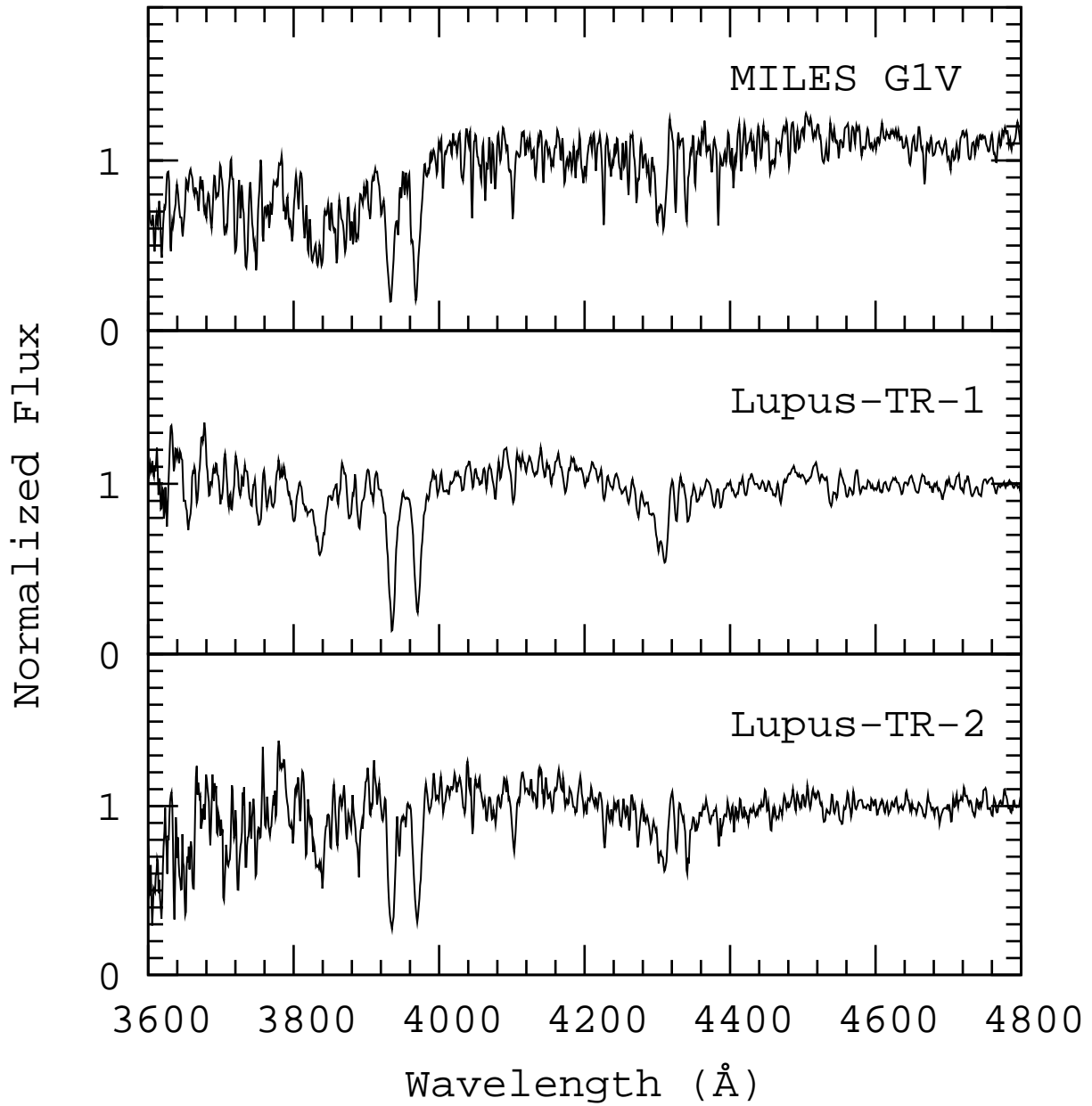


Fig. 6.— Spectra of a G1V from the MILES catalog (top), Lupus-TR-1 (middle), and Lupus-TR-2 (bottom). The spectra of the Lupus candidates were taken using the blue arm of the DBS on the ANU 2.3m telescope at SSO.

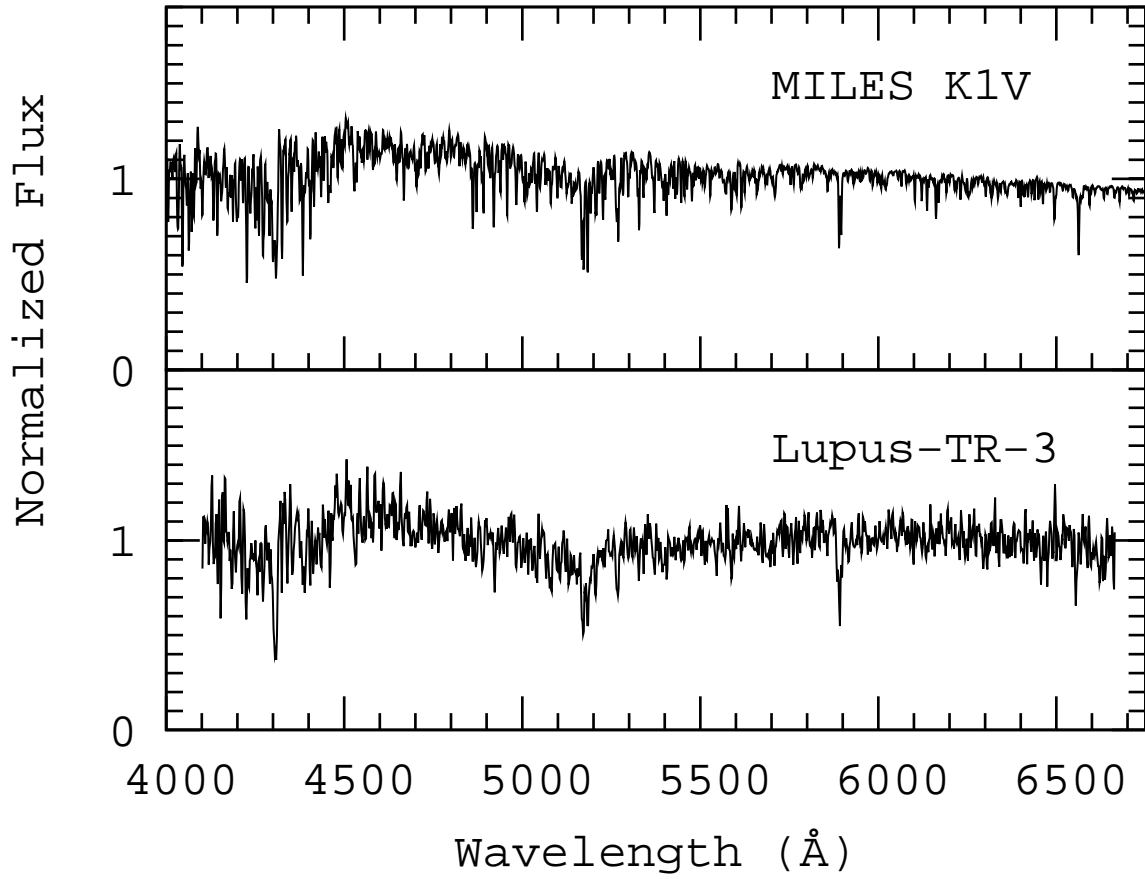


Fig. 7.— Spectra of a K1V from the MILES catalog (top) and Lupus-TR-3 (bottom). The Lupus-TR-3 spectrum was taken using the blue arm of the DBS on the ANU 2.3m telescope at SSO.

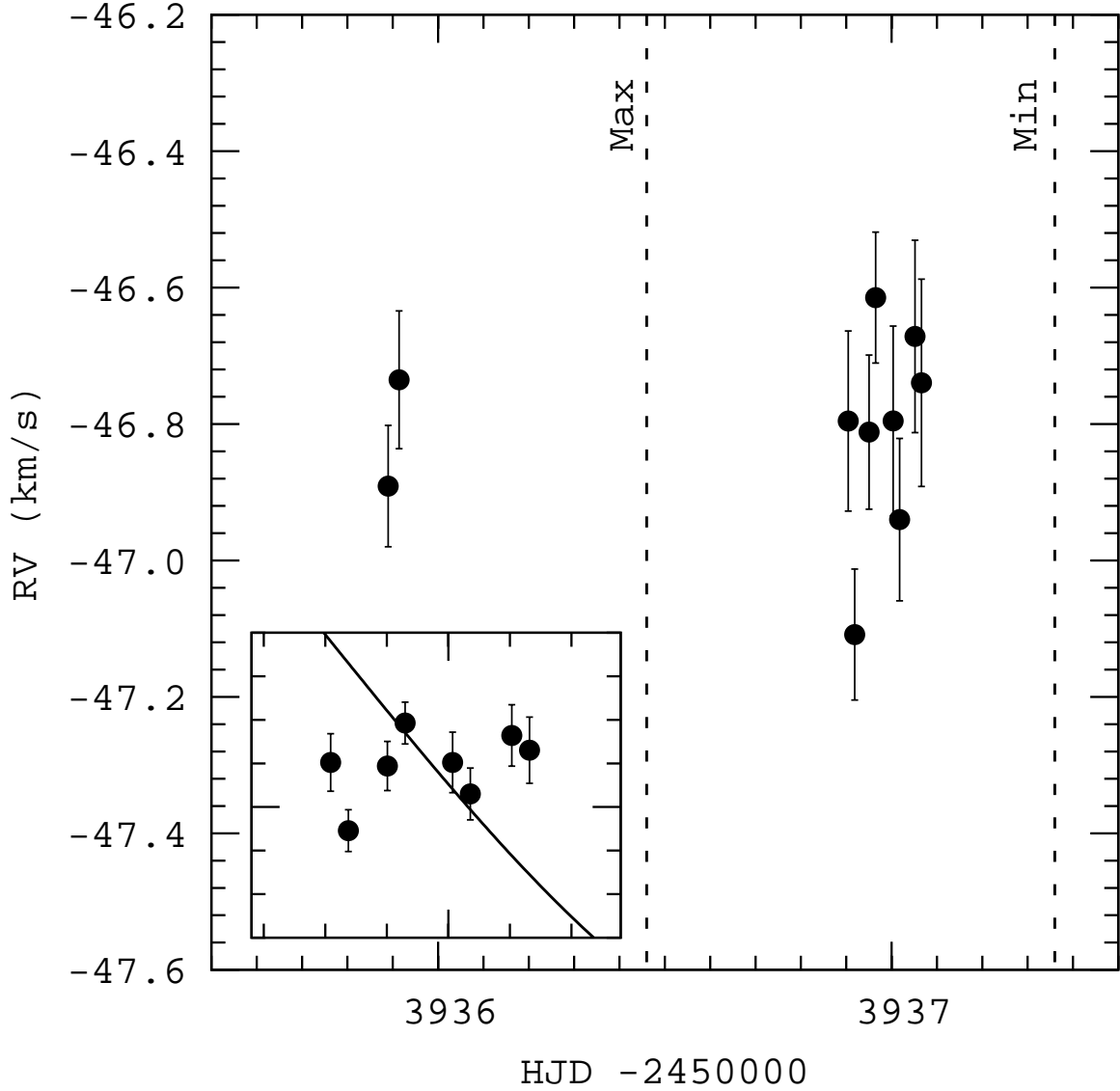


Fig. 8.— RV measurements for Lupus-TR-1 taken using UCLES on the AAT. The “Max” and “Min” dashed lines indicate the time of expected maximum and minimum RV variation. Inset: a magnified view of data from night 2 and a best fitting sine curve with $K = 2 \text{ km s}^{-1}$ (solid line). The data are clearly inconsistent with such an RV variation, indicating Lupus-TR-1 has no binary stellar companion with a 1.8 day period. It does not, however, rule out a blend scenario.

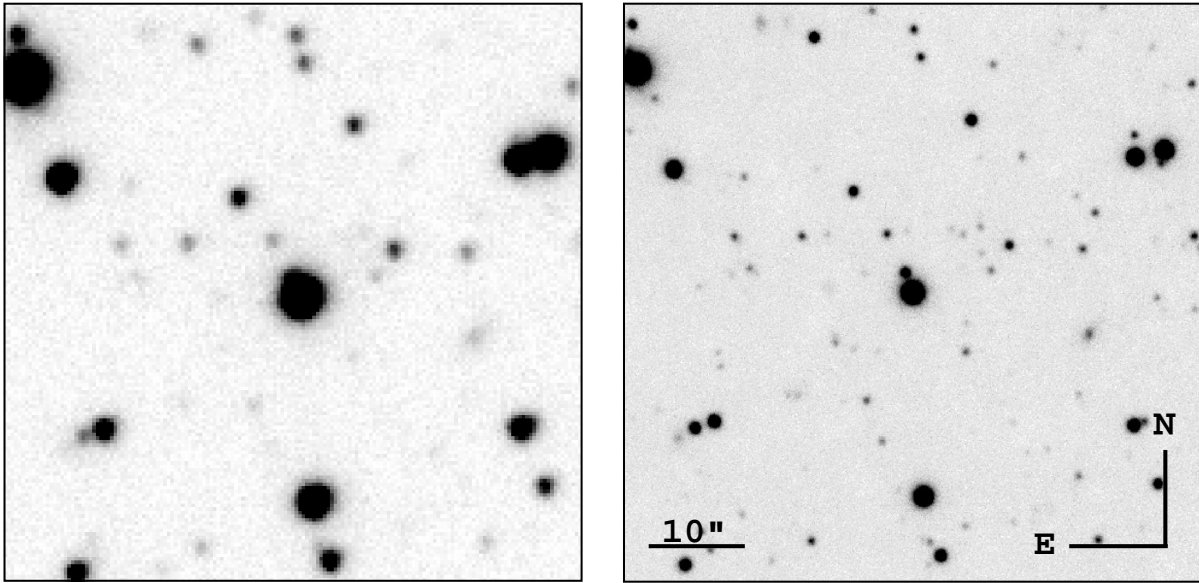


Fig. 9.— Left: image of Lupus-TR-1 (central star in frame) from WFI on the ANU 1 m telescope at SSO (FWHM=1.2 "). Right: image of Lupus-TR-1 taken with PANIC on Magellan I (Baade) (FWHM=0.65 "). The scale and orientation for both images are set out in the right panel. The neighbor is clearly resolved in the PANIC image NNE of Lupus-TR-1 with a separation of 2.3", and is very likely the blended source of the transit feature.

Table 1. Properties of the Lupus Transit Survey

Property	Lupus Transit Survey
Telescope	The ANU 40-inch telescope
Telescope Aperture	1 m
Telescope Site	SSO, Australia
Site Longitude	149.1° East
Site Latitude	31.3° South
Site Altitude	1150 m
Detector	The WFI
Detector Size (pixels)	8192 pixels \times 8192 pixels
Array configuration	Eight 2k \times 4k Lincoln Lab thinned CCDs
Pixel size (physical)	15 μ m
Pixel size (on sky)	0.375 "
Field of view	52' \times 52'
Readout time	\approx 50 s

Table 2. Candidate positions, magnitudes, colors, and spectral type

ID	RA (J2000.0)	DEC (J2000.0)	V	V–I	Spectral Type
Lupus-TR-1	15:30:51.6	-42:31:21.9	14.63	0.67	G1V
Lupus-TR-2	15:30:57.3	-42:59:02.4	14.78	0.63	G1V
Lupus-TR-3	15:30:18.7	-42:58:41.5	17.40	0.86	K1V
Lupus-TR-4	15:31:04.8	-42:57:10.3	16.33	0.77	...

Table 3. Candidate Properties

ID	Period (days)	Depth (d) (mag)	Duration T_{14} (hours)	T_C (HDJ-2450000)	η	S/N
Lupus-TR-1	1.81820	0.007 ± 0.006	4.98 ± 0.52	3525.998 ± 0.015	1.29	20.9
Lupus-TR-2	3.07070	0.020 ± 0.008	2.67 ± 0.10	3530.057 ± 0.072	1.02	26.3
Lupus-TR-3	3.91405	0.016 ± 0.004	2.65 ± 0.07	3887.092 ± 0.002	0.74	24.2
Lupus-TR-4	2.05398	0.013 ± 0.004	3.91 ± 0.12	3904.987 ± 0.022	1.23	23.2

Table 4. AAT RV Measurements for Lupus-TR-1

HJD (-2450000)	RV (km s ⁻¹)	$\pm 1\sigma$ (km s ⁻¹)
3935.890	-46.89	0.09
3935.914	-46.74	0.10
3936.904	-46.80	0.13
3936.919	-47.11	0.10
3936.950	-46.81	0.11
3936.965	-46.61	0.10
3937.003	-46.80	0.14
3937.018	-46.94	0.12
3937.052	-46.67	0.14
3937.066	-46.74	0.15